

SCALABILITY ANALYSIS OF RADICAL TECHNOLOGIES TO VARIOUS AIRCRAFT CLASS - PART II: SENSITIVITY ANALYSIS

Vincent O.Bonnin¹ & Maurice F.M. Hoogreef²

^{1,2}Faculty of Aerospace Engineering, Delft University of Technology, Delft, the Netherlands

Abstract

This study aims at providing a landscape of opportunities and limitations for hybrid-electric aircraft (HEA) and hydrogen-powered aircraft by investigating several technological combinations applied to three aircraft classes: Regional (REG), Short-Medium Range (SMR) and Large Passenger Aircraft (LPA). The preliminary sizing of HEA using different hybrid-electric powertrain architectures, combined with various distributed propulsion layouts is conducted. The resulting HEA are then compared to a conventional design, on the basis of several performance metrics, for variations in harmonic range and passenger capacity. Throughout the design space considered, it is found that opportunities for radical aircraft design are scarce and offer limited prospective.

Keywords: hybrid-electric; scalability; preliminary design; hydrogen

Nomenclature

AR	=	Aspect Ratio (wing) (\sim)	MTOM	=	Maximum Take-Off Mass (t)
BLI	=	Boundary Layer Ingestion	MZFM	=	Maximum Zero Fuel Mass (t)
BM	=	Battery Mass (t)	NA	=	Not Applicable
b	=	Wing span (m)	OEM	=	Operative Empty Mass (t)
C_{Di}	=	Induced drag coefficient (\sim)	P	=	Power (kW)
CHYLA	=	Credible Hybrid Electric Aircraft	P1	=	Primary propulsor/powertrain
C_L	=	Lift coefficient (\sim)	P2	=	Secondary propulsor/powertrain
Com	=	Commuter	PAR	=	Parallel
CS	=	Certification Specification	PM	=	Payload mass (t)
d_{fus}	=	Fuselage diameter (m)	PREE	=	Payload Range Energy Efficiency (\sim)
E	=	Energy (GJ)	PTE	=	Partial Turbo Electric
EoM	=	Equations of Motion	R	=	Range (km)
FM	=	Fuel Mass (t)	REG	=	Regional Aircraft
GA	=	General Aviation	S	=	Wing area (m^2)
H2	=	Hydrogen	SMR	=	Short/Medium Range aircraft
h_{cr}	=	Cruise altitude (m)	SPPH	=	Series-Parallel Partial Hybrid
LEDP	=	Leading Edge Distributed Propulsion	T	=	Thrust (kN)
LH ₂	=	Liquid Hydrogen	T/W	=	Thrust to Weight ratio (\sim)
LPA	=	Large Passenger Aircraft	TF	=	Turbo fan
l_{fus}	=	Fuselage length (m)	TLAR	=	Top Level Aircraft Requirement
M_{cr}	=	Cruise Mach number (\sim)	TP	=	Turbo prop
MDO	=	Multidisciplinary Design Optimization	W/P	=	Power loading (kN/kW)
			W/S	=	Wing loading (kN/m^2)
			WtipMP	=	Wing Tip Mounted Propulsion

1. Introduction

Since the dawn of commercial aviation in the 1950s, improvements in the order of 80% have been achieved in terms of vehicular energy consumption per unit mass transported over a unit distance. However the multi-fold increase in annual transported passenger-miles has still driven the ecological footprint of aviation up over the last 60 years [1]. To curb this trend, aggressive emissions reduction targets have been set by various international institutions [2, 3], which call for the investigation of disruptive technologies to be adopted in aircraft designs. In this context, over the past decade, numerous research works have been conducted in the field of Hybrid Electric Propulsion (HEP), usually combined with distributed propulsion (DP), in order to probe the prospects of such technology in coping with those drastic emission reduction targets.

So far, those research initiatives typically address either a single vehicle or vehicle class [4] or a single technology [5]. Yet the relative performance variations entailed by a given technology are intrinsically dependent on the Top-Level Aircraft Requirements (TLARs) associated with a given vehicle class. Therefore, the community is still lacking a comprehensive view of the opportunities and limitations offered by the application of key radical hybrid-electric technologies over the various aircraft classes, as a function of the technology assumptions made. Such an overview is of prime importance to understand which radical aircraft could fly first and how the maturation of the technology they employ would drive their evolution towards different scales and wider usages. This current investigation fulfills the objective of the EU-funded project CHYLA (*Credible HYbrid eLectric Aircraft*) that is funding the present research work.

The objective of the present study is to outline a landscape of technology application and identify areas suitable for scaling, as well as limitations or challenges for development. This landscape is formed by variations in selected Key Performance Indicators (KPIs) over a space of variables that include aircraft requirements, and technology combinations. The resulting topography will outline favorable areas and the conditions to their extension over a larger domain.

A preliminary design tool tailored for the generic sizing of hybrid electric aircraft is used to explore sensitivities to harmonic range and passenger capacity within each of the following aircraft class: Regional (REG), Short-Medium Range (SMR), Large Passenger Aircraft (LPA), for a pre-determined set of HEP architectures and DP layout. The present research output comes as a continuation of the parallel article from Hoogreef et. al [6], which focuses on the sizing and analysis of initial design aircraft, within each of the above class.

2. Aircraft Conceptual Design

2.1 Aircraft Sizing Tool

The tool used for the preliminary sizing of the HEP aircraft considered in this study, called the Aircraft Design Initiator (or simply *Initiator*), is detailed in the *Part I* of this study [6]. It has been developed in-house at TUDelft [7] and is the object of continuous improvements. This software, which was initially conceived for the conceptual design of both conventional and unconventional aircraft configurations (eg: blended wing body and box-wing) has been modified in recent years to enable the analysis of HEP aircraft fitted with various DP layouts [4]. It consists overall in successive convergence loops on Maximum Takeoff Mass (MTOM), nested within each other and of increasing analysis fidelity, which iteratively alter high-level design variables to eventually converge towards an aircraft design that abides by the given set of input TLARs. Figure 1 shows the process at an aggregated level.

Powertrain modelling as well as aero-propulsive interactions are accounted for in the Class I iterative process, via a generic sizing method suited especially for hybrid-electric aircraft with distributed propulsion. In particular, it differs from the traditional sizing methods by accounting for aero-propulsive interaction effects and by including a powertrain model capable of dealing with power shares that may differ along the mission phases.

In a nutshell, constraints of the design-selection diagram, which stem from equations of motion (EoM) of a simplified point-mass aircraft, account for the way wing aerodynamics and propulsion interact (DP-layout dependent) via aero-propulsive models.

The power split within the powertrain architecture considered can be modified for each constraint, or flight phase considered, via so-called *power control parameters*, see Section 2.2.2 For instance,

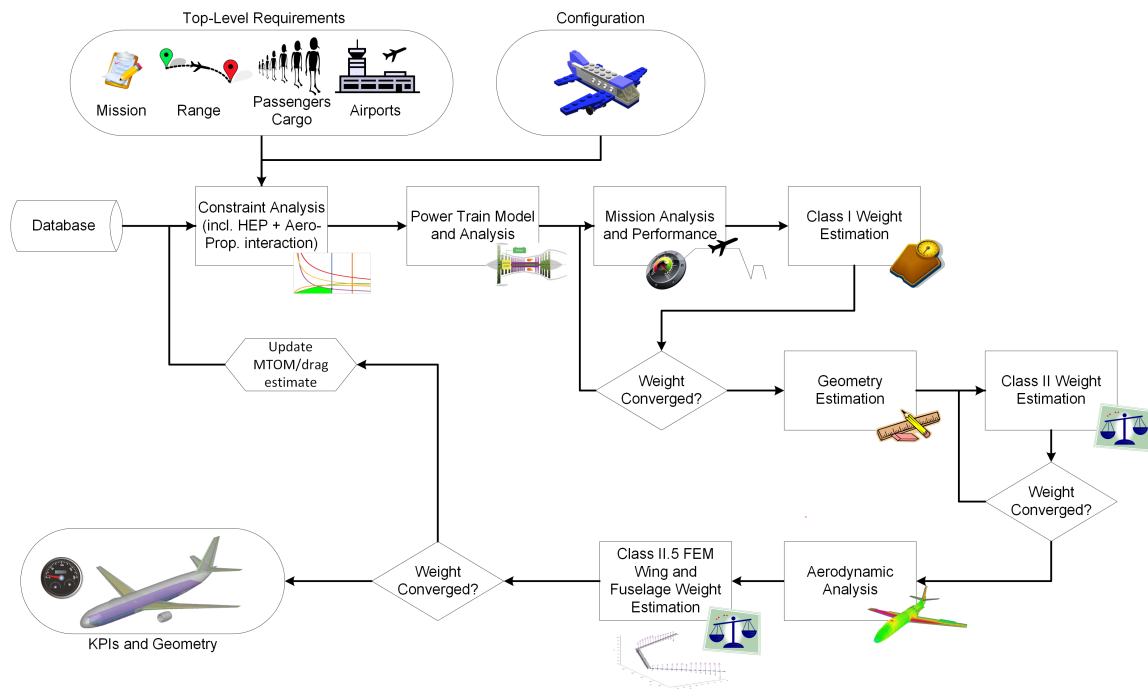


Figure 1 – Illustration of the *Initiator* process flow, for the design of hybrid electric aircraft, from [8]

battery power supply can be set for take-off and climb only and be switched off in cruise. Those combined constraints give shape to a feasible design space. A design point must be selected (eg: max wing-loading, max gas turbine power-loading) to provide the associated wing-loading and power-loading for each component of the powertrain. Those enable to size wing and powertrain components for a given take-off mass. Masses of energy-related components are subsequently obtained from a Mission Analysis module that runs an integration scheme on the EoM of a point-mass aircraft along each flight phase to compute the respective energy needs. If the process converges, the obtained vehicle is only one among a virtual infinity of feasible aircraft within the same constrained design-space. The design point is not selected by an optimizer, but rather is an a-priori design choice informed by engineering know-how. Various other variables are to be set by the user, in order to keep control of the design directions.

2.1.1 Powertrain Modeling

The modeling of powertrains is formed of variations around a simplified conceptual representation of components and power flows. Powertrain architectures are composed of a "primary" powertrain which gathers all components that are mechanically linked to the gas turbine and of a "secondary" powertrain which includes components of the electrically-driven propulsion system.

One significant assumption is that the gas turbine power output is composed of the mechanical power on its shaft only. In other words, the GT core itself does not provide any propulsive power. If that assumption holds for turbo-propeller or turbo-shaft architectures, it however is quite erroneous for turbofan designs, where the core provides a non-negligible fraction of the thrust.

Besides, powertrain components are not modeled, but rather have their properties a-priori assumed. This allows to reduce the computational time and provides the ability to directly control key-governing variables.

The case of hydrogen-powered aircraft involves conventional powertrain layouts but requires dedicated work on the sizing and integration of the liquid hydrogen tank [9], and of the fuel-cell [10] if that applies.

The *Initiator* does not use a GT model, but an user-assigned value for GT thermal efficiency (see last row off table 5), then down-rated by a thermal efficiency lapse parameter, function of gas turbine throttle and operating Mach. Therefore the impact of operating conditions and eventual power off-take on GT performance is accounted for in a simplistic way within the *Initiator*. Therefore, for *parallel*

powertrain architectures where the use of hybridization aims at down-sizing the gas turbine to its on-design operating conditions, albeit aircraft-level improvements were proven to be hardly realizable [11], results from the *Initiator* are exposed to significant error margin.

2.1.2 Aero-Propulsive Interactions

The *Initiator* is able to account for the aero-propulsive interactions of a large variety of propulsion layouts via several available low-fidelity aero-propulsive models. Most of those are surrogate models built on a set of results from aero-propulsive models of higher fidelity, each adapted to a given propulsion layout. Therefore, they are by essence reduced-order models that account for the main aerodynamic phenomenon entailed by a given propulsion layout, for a limited range of operating conditions. In the present study, the so-called 'LLM' model used for most designs, eventually in combination with the 'BLI' model, is based on a VLM approach [12] which accounts for the propeller swirl and axial induced velocity with the following limitations:

- the impact of the wing on the propeller is ignored.
- the axial slipstream height is virtually 'infinite' along the propeller radius, which leads to an over-prediction in wing lift-coefficient. This limitation is currently being improved at TUDelft.

2.1.3 Aero-Structural Model

The sizing of the fuselage and of the wing primary structure is done within the Class 2.5 loop of the *Initiator*, via simplified finite-element methods. Concerning the wing, load cases account for the discrete loads of engine and wing-mounted components but not for aero-propulsive interactions, such that the aerodynamic loads are that of a 'clean' wing, without any propeller interaction. This approximation was shown to be acceptable [13] with only a minor impact on wing mass (below 1%) . Overall, the *Initiator* should not be comprehended as a tool for the quantitative estimation of KPIs. But it is suited to rapidly produce aircraft designs and explore relative trends between different design. As such, the performance metrics of resulting hybrid-electric aircraft designs should be analyzed relatively to their so-called 'baseline' counterparts: aircraft designs obtained with the same methodology subject to the same TLARs, but with a conventional combination of powertrain and propulsion layout.

2.2 Technology Combination

A radical aircraft configuration is defined by a given set of TLARs, by a given airframe configuration (eg: planform and location of aero-surfaces) and by the following technical combination: nature of the energy carriers envisioned for flight, powertrain architecture and propulsion layout. The following options are being considered for each of those categories:

- energy carrier: fuel, fuel and battery, battery
- powertrain architecture: Conventional, Serial, Parallel, Serial/Parallel Partial Hybrid (SPPH), Partial Turbo Electric (PTE), Turbo-electric, Full electric (see figure 2)
- propulsion layout: Conventional, Leading Edge Distributed Propulsion (LEDP), Wing-mounted Tip Propellers (WMP), Boundary Layer Ingestion (BLI)

Figure 2 displays the various powertrain architectures options. Not all are considered in the present study.

Part I of this study [6] details the down-selection conducted out of the total possible combinations to obtain those investigated in this study. To summarize, some combinations are not simply not feasible. For instance, a parallel powertrain does not support a secondary propulsion layout. Then some technologies can already be excluded for certain categories based on previous research. For instance it was chosen to exclude the turboelectric powertrain given its limited prospects [4], although it remains a specific case of the PTE. Besides, based on results about the debilitating impact of high degrees of hybridization [5], it was deliberately chosen to not consider full-electric aircraft at the scales considered. Furthermore, it was decided to only consider the technology combinations with

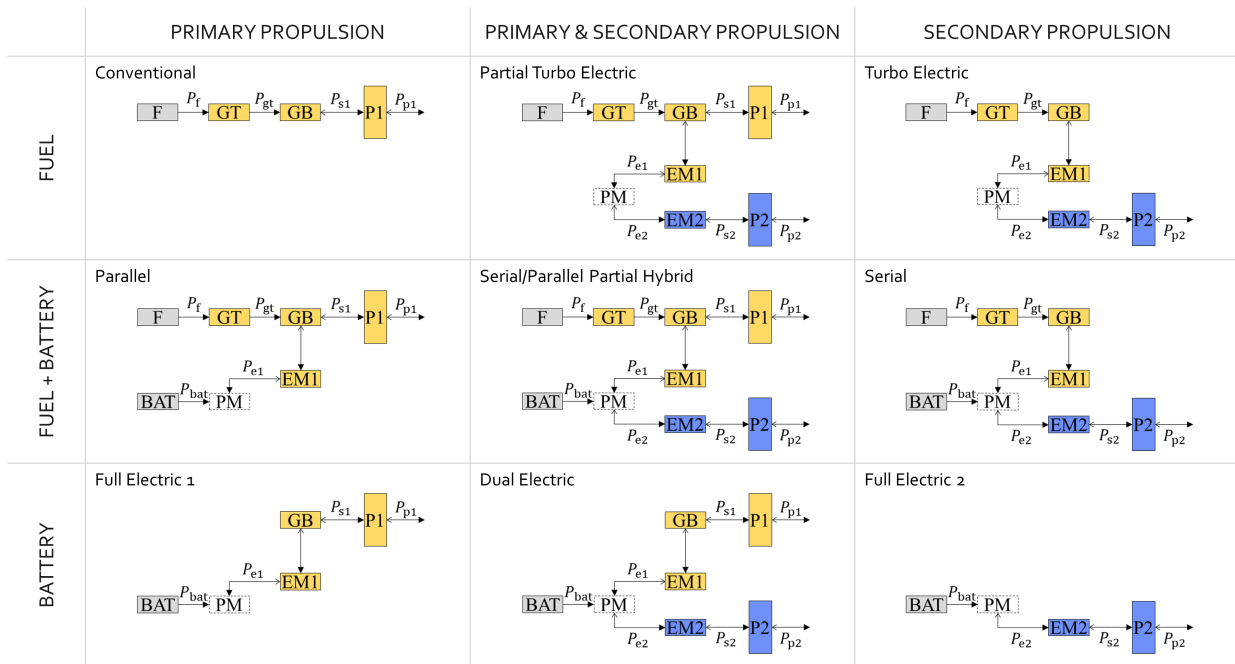


Figure 2 – Notional representation of powertrain architectures, adapted from [14]. "F" and "BAT" refer to fuel and battery respectively. As for components, "GT" stands for Gas Turbine, "GB" for Gear Box, "EM" for Electric Motor, "PM" for Power Management and "P" for propulsor. Upper-case letters are used for energy sources and powertrain components, while power paths are indicated with lower-case subscripts, with arrowheads indicating the feasible direction of the power flow

the highest prospects and credibility within each respective aircraft class, based on previous research as well as engineering know-how.

An overview of the selected combination is displayed in fig.3. On top of the those radical aircraft configurations, aircraft of conventional powertrain architecture and propulsion layout and called 'baseline', are also sized with the *Initiator* in each of the three classes. Those aircraft abide by the same TLARs and serve as benchmark for radical aircraft, for a given set of TLARs.

	Partial Turbo Electric	Parallel	Serial Parallel Partial Hybrid
FUEL	P1: TF. P2: BLI-fan LPA; SMR		
	P1: TP. P2: BLI-fan Reg		
	P1: TP. P2: WMP Reg		
FUEL + BATTERY		P1: boosted TF. P2: NA SMR	P1: TP. P2: BLI-fan Reg
		P1: boosted TP. P2: NA Reg	P1: TP. P2: WtipMP Reg

Figure 3 – Combinations in energy source and powertrain architectures, for different aircraft classes and propulsion layouts, selected for the present work. P1 and P2 refer to primary and secondary propulsion respectively. The propulsion layout considered are TurboFan (TF), TurboProp (TP), Boundary Layer Ingestion (BLI fan) and Wing tip Mounted Propeller (WMP), while "NA" refers to Non Applicable. In colored letters, aircraft classes populate the table.

2.2.1 Variations in TLARs

Part I of this study [6] identifies three aircraft classes, which all fall under the CS-25 regulatory framework, and assigns each with a set of TLARs. TLARs values adopted within each class are inspired from reference real-world aircraft and summarized in fig.4. The ATR72-600, the Airbus A320NEO, and the Airbus A350 were selected as reference aircraft for the class REG, SMR and LPA respectively: the initial values of TLARs in each class are slightly adapted from those.

		LPA (~A350-900)	SMR (~ A320-NEO)	Reg (~ ATR72-600)
TLARs	pax	315	150	70
	payload [t]	53,5	20	7,5
	range [nm / km]	5 830 / 10 800	2 560 / 4 555	500 / 926
	cruise Mach	0,85	0,78	0,4
	cruise alt [ft / m]	40 000 / 12 192	37 000 / 11 278	23 000 / 7 010

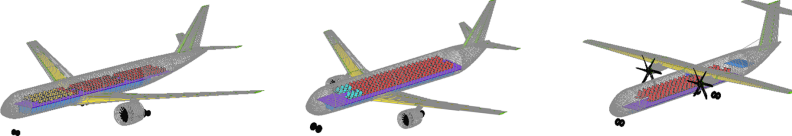


Figure 4 – Summary of TLARs over the three transport aircraft classes, together with a representation of the sizing respectively obtained with the *Initiator*

It is worth noting that the TLARs of such reference aircraft result from the analysis of technical and economic trends conducted by airframers in order to outline best market opportunities. However, in the present study, costs are not modeled and therefore key economic trends are missing. For instance, the cruise speed and the range directly affect the mission flight time, which has an impact on the economics of the flight by affecting revenue (via demand and volume of pax.km flown per day), and costs (eg: crew cost per trip). By limiting itself to technical-related KPIs, the present study therefore only provides partial insights into the competitiveness of radical aircraft against conventional ones.

The TLARs that are varied in this paper are the harmonic range and the passenger capacity. They are varied separately such that when one is being altered, the other remains constant at its initial value. All other TLARs are fixed, see Table 1 in *Part I* [6] for more details.

The passenger capacity directly affects the cabin floor area and the payload mass. For the cabin floor area, the passenger distribution per cabin class is kept around the values assumed for the initial aircraft, see fig.4. Yet small variations are allowed to ensure that each seat row is completely filled, such that the overall floor area passenger density would not vary much when the overall passenger capacity is changed. For the sake of simplicity, the seating layout (pitch, width, etc...) of each cabin class is kept identical, including the numbers of seats abreast, which determines the fuselage width. This arbitrary choice is probably not optimal from a design point of view (SMR aircraft of passenger capacities from 100 to 140 would probably be lighter with 5-abreast seating in economy class than with 6). Besides, the available cabin length and cabin seating layout are typically assessed in conjunction within the preliminary design phase so as to minimize the number of required emergency doors. This consideration was not taken into account when deriving the values of passenger capacity considered here, such that the number of exit door is adapted from the given cabin layout.

Regarding the payload mass, the overall passenger mass is obtained from an assumed 100kg mass per headcount (80 kg passenger and 20 kg luggage) and the cargo mass is adapted such that the ratio of passenger mass to cargo mass is kept constant.

Variations in TLARs explored within this study are summarized in Table 1 and Table 2. The intervals in range and passenger capacity are established to be representative of each respective class (eg: SMR passenger capacity approximately in the 100-200 interval).

Table 1 – Variations in harmonic range for each aircraft class. In bold are the initial values.

Aircraft Class	Harmonic Range [km]					
REG	556	741	926	1111	1296	1482
SMR	2733	3188	3644	4099	4555	5010
LPA	6480	7560	8640	9720	10800	11880

Table 2 – Variations in passenger capacity and corresponding payload mass for each aircraft class. In bold are the initial values.

Aircraft Class	[Pax capacity [-]; Payload Mass[tons]]					
REG	[50; 5.4]	[60; 6.4]	[70; 7.5]	[80; 8.6]	[90; 9.6]	[100; 10.7]
SMR	[104; 13.9]	[122; 16.3]	[150; 20]	[174; 23.2]	[196; 26.1]	
LPA	[269; 45.7]	[294; 49.9]	[315; 53.5]	[337; 57.2]	[362; 61.5]	

Previous research [5] has underlined the importance of cruise altitude in the comparison between aircraft design: radical and baseline aircraft are likely to exhibit different optimum altitudes, due to the increased wing-loading enabled by distributed propulsion. In the present case, the distributed propulsion layout considered, WtMP and BLI, do not alter the feasible wing loading or marginally. Overall, it was decided not to change the cruise altitude between baseline and radical aircraft.

2.2.2 Design Guidance and Parameters

For all aircraft considered in this study, the selected design point (cf Section 2.) is based on the criteria of maximum wing loading. This design point is known to produce the lowest MTOM for conventional aircraft [15] and also minimize MTOM for radical aircraft [5].

Depending on the powertrain architecture, up to three so-called *power control parameters* (PCP), defined in Equations 1, 2 and 3 below, can be necessary to determine the power flow within each component. The *supplied power ratio*, see [5, 16], is expressed as the ratio of battery supplied power to the total supplied power.

$$\Phi = \frac{P_{bat}}{P_{bat} + P_f} \quad (1)$$

The second power control parameter is the *shaft power ratio*, defined as the ratio of the mechanical shaft power supplied to the secondary propulsion layout to the total shaft power produced by the powertrain.

$$\varphi = \frac{P_{s2}}{P_{s1} + P_{s2}} \quad (2)$$

Finally, the *gas turbine throttle* parameter, expressed in Equation 3 represents the power fraction at which the gas turbine is operating, as the ratio of produced power to the maximum power it can produce in the given flight condition.

$$\xi = \frac{P_{GT}}{P_{GTmax}} \quad (3)$$

Table 3 – Power control parameters input values used for radical design where it applies. Except for the baseline aircraft included for the sake of comparison, other non-DP radical aircraft are not included. Pairs correspond to respective values of PCP at the beginning and end of the considered mission analysis phase. Cells are left empty when PCP are non-applicable. 'TbD' refers to values that are not input but left to compute by the Class 1 loop of the *Initiator*.

Aircraft	MA flight phase	GT throttle ξ	Supplied Power Ratio Φ	Shaft Power Ratio φ
REG-baseline	Climb	0.70-0.95		
	Cruise	0.90-0.90		
	Descent	0.035-0.035		
REG-boosted	Climb	0.90-0.90	0.00-0.05	
	Cruise	0.85-0.85	TbD-TbD	
	Descent	0.25-0.10	0.00-0.00	
REG-PTE-BLI	Climb	0.70-0.95		0.00-0.00
	Cruise	TbD-TbD		0.08-0.08
	Descent	0.035-0.035		0.00-0.00
REG-PTE-WtMP	Climb	0.70-1.00		0.10-0.14
	Cruise	TbD-TbD		0.20-0.20
	Descent	0.035-0.035		0.00-0.00
REG-SPPH-BLI	Climb	0.90-0.90	0.01-0.05	0.07-0.05
	Cruise	0.90-0.90	TbD-TbD	0.05-0.05
	Descent	0.05-0.05	0.00-0.00	0.05-0.05
REG-SPPH-WtMP	Climb	0.90-0.90	0.01-0.05	0.08-0.18
	Cruise	0.90-0.90	TbD-TbD	0.20-0.20
	Descent	0.05-0.05	0.00-0.00	0.00-0.00
SMR-baseline	Climb	1.00-1.00		
	Cruise	0.90-0.90		
	Descent	0.035-0.035		
SMR-boosted	Climb	0.90-0.90	0.08-0.10	
	Cruise	0.90-0.90	TbD-TbD	
	Descent	0.05-0.05	0.00-0.00	
SMR-PTE-BLI	Climb	1.00-1.00		0.02-0.07
	Cruise	TbD-TbD		0.08-0.08
	Descent	0.035-0.035		0.00-0.00
LPA-baseline	Climb	1.00-1.00		
	Cruise	0.85-0.85		
	Descent	0.05-0.05		
LPA-PTE-BLI	Climb	1.00-1.00		0.02-0.07
	Cruise	TbD-TbD		0.08-0.08
	Descent	0.05-0.05		0.00-0.00

Power control parameters can be set to different values for different flight phases, such that climb can use a different power split compared to cruise or descent. By affecting the power-related sizing within each branch of the powertrain and the energy needs along the mission, those *power control parameters* have a significant impact on design. Lessons learnt from previous studies were applied for the selection of PCP:

- When battery is used as an energy carrier, a high supplied power ratio Φ has a debilitating impact on aircraft performance, see Figure 7 of [5]. In the present study, battery power output is only positive during climb to lower the power loading of the gas turbine and help it maintain a constant throttle ξ of maximum efficiency throughout the entire climb phase. During cruise and descent, Φ is chosen such that either the battery power output is null or slightly negative (excess power from the GT channeled to the battery during cruise as the aircraft gross weight and energy needs decrease).
- Values of shaft power ratio equal to or lower than 0.20 only are beneficial [17]. Above those values, power losses and increased weight in electrical components exceed the eventual benefits in aero-propulsive efficiency. Besides, channeling more shaft power towards the secondary propulsion may lead to a decrease in propulsive efficiency due to the increased disk loading.
- In the case of a BLI system, if the propulsive power exceeds the amount of power dissipated in the fuselage boundary layer, the associated propulsive efficiency would start to decrease, such that a theoretical limit exists regarding values of ϕ associated with a benefit.
- In the case of a WtipMP system, values of ϕ around 0.1-0.2, associated with values for the span fraction covered by the propulsion system of around 20 percent, lead to the most interesting improvements [13]. For all aircraft with wing-tip mounted propellers as a secondary propulsion layout, a maximum shaft power ratio of 0.20 and a span fraction of 0.30 are used.

Table 3 summarizes the values in PCP used throughout the present study. It can be seen that for aircraft equipped with battery, the GT throttle is kept at a constant level during climb and cruise, as the battery provides the excess power required to climb. Besides, during cruise, the supplied power ratio is left to be determined by the *Initiator* to match the required flight condition (altitude, Mach) at the aircraft gross weight, for the values of GT throttle that are set by the user. Setting both parameters for given flight conditions would lead to an over-constrained system of equations (power conversion and power split equations for the powertrain, equations of motion for the aircraft). Similarly, for PTE configurations during cruise, the GT throttle is adapted by the *Initiator* to match flight conditions for a given value of ϕ .

Assumptions regarding power-electronics parameters have a direct and significant impact on aircraft-level performance. The value used for all HEA in this study are listed in table 4.

Table 4 – Values of power-electronics parameters used in this study

Component	Parameter	Value	Units
Battery (pack-level)	gravimetric power density	1750	[W/kg]
	gravimetric energy density	437.5	[Wh/kg]
	volumetric mass density	2615	[kg/m ³]
	minimum state-of-charge	20	[%]
Electro-Motors (includes cooling systems, power management inverter, rectifier)	gravimetric power density	2625	[W/kg]

Besides, table 5 summarizes the constant values for efficiency assumed in the present study.

Table 5 – Values of component efficiency used in this study

Component	Symbol	Value
Electro-Motors	η_{EM}	0.95
Power Management and Distribution	η_{PM}	1.00
Gearbox	η_{GB}	0.95
Gas turbine (before efficiency lapse)	η_{GT}^*	0.42

2.2.3 Key Performance Indicators

The aircraft-level KPIs that are being monitored along the sensitivity analysis are listed below, together with an eventual description:

- *MTOM*
- *OEM*
- *PREE: Payload Range Energy Efficiency*, defined in [5] as $PREE = PL.R/E_{mission}$, with PL the payload mass, R the mission range and $E_{mission}$ the total energy consumed along the mission. In the remainder of this paper, the *PREE* is computed with respect to the energy spent during the nominal mission, excluding loiter and diversion.
- $\eta_p.L/D$: *aero-propulsive efficiency*, defined in [17], with L/D the lift-over-drag ratio and η_p the overall propulsive efficiency, defined by: $\eta_p = (1 - \varphi) \cdot \eta_{p1} + \varphi \cdot \eta_{p2}$, with φ the *shaft power ratio* defined in eq. 1. The *aero-propulsive efficiency*, in steady level flight can be related to the shaft power via the following equation: $\eta_p.L/D = v.W/(P_s)$. It can be comprehended as the efficiency at which the aircraft converts a given shaft power-to-weight ratio P_s/W into useful velocity v .
- E_f : fuel energy consumed along the nominal mission, excluding loiter and diversion. It is representative of the CO2 emitted by the aircraft to complete its mission.

It should be noted that KPIs are not expected to be unilaterally better or worse between two designs, such that aircraft comparisons may be relative to the KPI considered. It would be of great interest to compare a pair of KPIs provided that others are constant. For instance compare the *PREE* for two aircraft configurations with similar CO2 emissions over the mission. But this requires extra degrees of freedom to be included in the sensitivity analysis and sufficient related sampling points over those, probably via a design of experiment approach.

3. Range Exploration

3.1 Regional Aircraft

The variation in aircraft MTOM required to fulfill the harmonic mission with varying range is displayed for regional aircraft in fig.5. The harmonic mission requires to fly the maximum payload over a given harmonic range, including reserves.

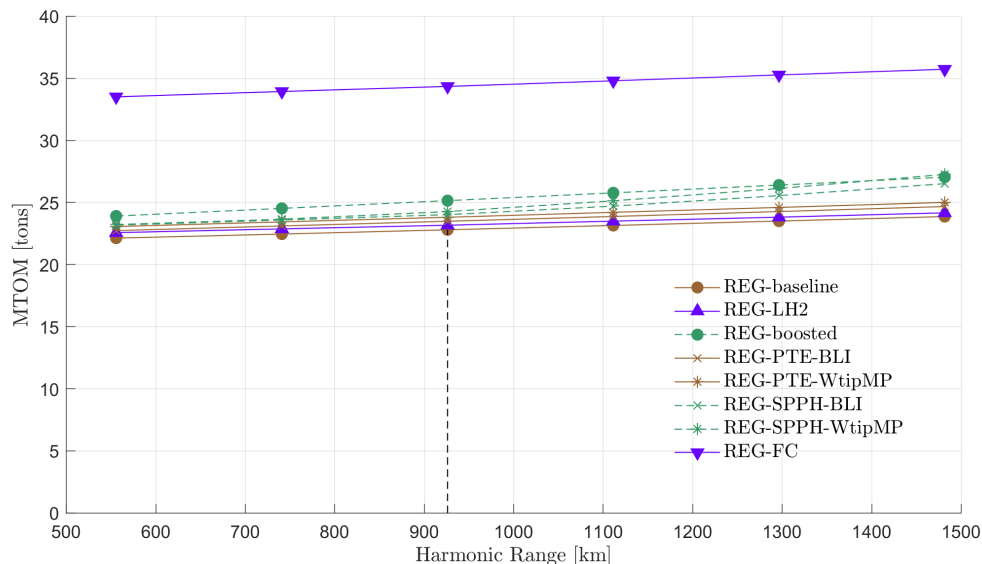


Figure 5 – Evolution of MTOM with varying harmonic range for the Regional class. The vertical dashed line indicates the initial range value

A first observation concerns the outlying MTOM values of the *REG-FC* fuel-cell aircraft, even though the relative difference with the *REG-baseline* MTOM decreases from 50% to 44% along the interval of harmonic range considered. It is chosen to discard the fuel-cell option in the following analysis with the conclusion that the low gravimetric power density of fuel-cell systems and their associated batteries is not a viable option for aircraft of the regional class.

Figure 6 offers a more detailed insight into MTOM variations with harmonic range and also displays the evolution of PREE over the same interval. Aircraft equipped with batteries, in green color on 6, are the heaviest. All aircraft see their MTOM increase in a pseudo-linear way with harmonic range, with the exception of the two *REG-SPPH* configurations. Those are just marginally heavier than their *REG-PTE* counterparts for the lowest ranges, but compare to the heaviest *REG-boosted* variant for longer ranges.

For those aircraft, values in supplied power ratio during climb and cruise are determined such that the GT throttle is constant while the battery is discharging during climb and recharging during cruise (at a significantly lower rate). If climb discharge and cruise recharge balance out, which is approximately the case for the initial 500nm range considered, recharging the battery during cruise does not alter the battery mass, but costs a few percent of GT power to ensure the battery is ready to be used for next flight. For the lowest range values, the cruise is shorter and the recharge only accounts for 35% of the battery energy spent to climb, which means that ground recharge must be conducted but does not change the battery capacity. However, for harmonic ranges above the initial 500 nm value, the recharge can represent up to 300% of the battery discharge, and the battery capacity increases to accommodate that charge.

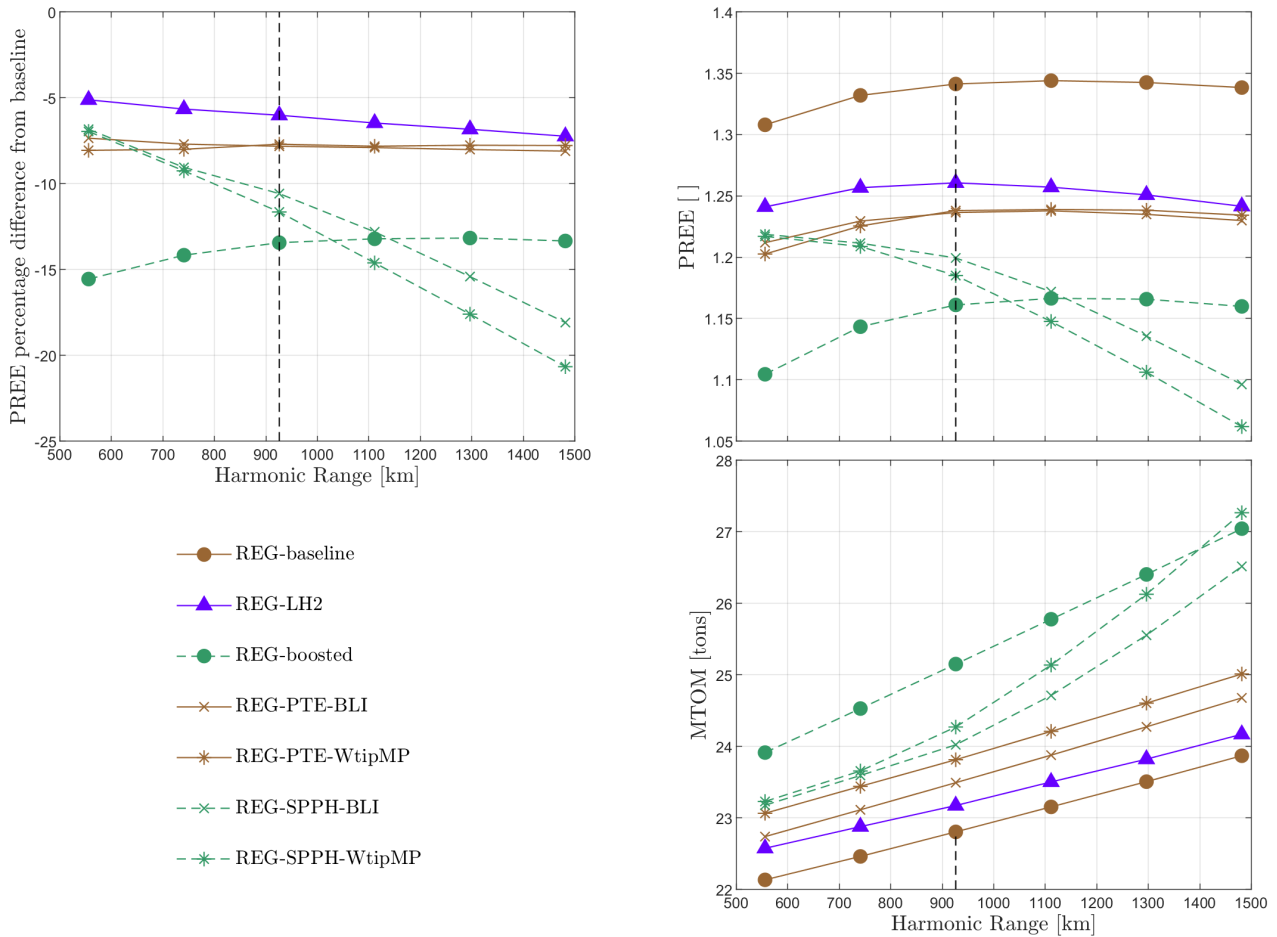


Figure 6 – Variations in MTOM and PREE with harmonic range. The vertical dashed line indicates the initial range value

This 'over-charging' phenomenon only happens from a certain range, which is quite evidently displayed on the MTOM curves of the two *REG-SPPH* aircraft. There are several ways around this over-sizing of the battery. One would be to adapt the GT throttle in cruise such that the cruise recharge just balances out the climb discharge, but that would possibly require a higher GT power loading at smaller harmonic range. Not to mention that most of the mission performed by an aircraft are over ranges below the harmonic range. Another option would be to impose a recharge during the descent, such that it would be much less sensitive to the traveled range. Finally, a last alternative is to allow discharge only and have a 'plug-in hybrid' aircraft. That option requires the transformation of airport infrastructures to allow fast recharging during the turnaround time.

A general observation that can be made from fig.6 is that overall aircraft of increasing PREE display a decreasing MTOM. Besides, for the whole interval in range considered, no radical aircraft is able to match the efficiency of the *REG-baseline* aircraft, or even able to come within 5% of its PREE level. This outlines that the eventual system-level improvements brought by radical technology combinations are of second order compared to the influence of mass on aircraft-level performance.

3.2 Short-Medium Range Aircraft

The variation in aircraft MTOM required to fulfill the harmonic mission with varying range is displayed for SMR aircraft in fig.7. The harmonic mission requires to fly the maximum payload over a given harmonic range, including reserves.

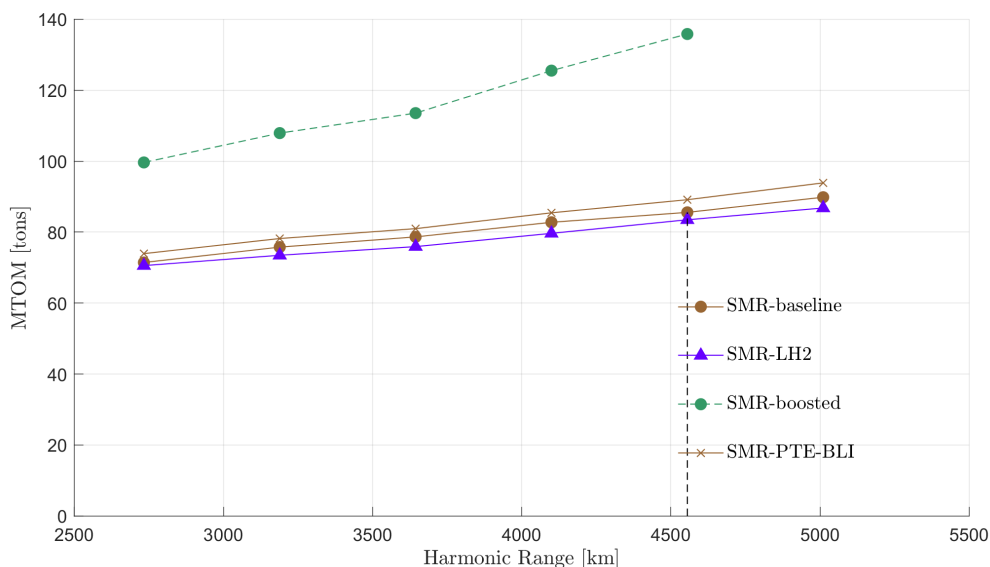


Figure 7 – Evolution of MTOM with harmonic range for the Short-Medium Range class. The vertical dashed line indicates the initial range value.

A first observation concerns the debilitating impact of battery on MTOM. The *SMR-boosted* exhibits an MTOM penalty of at least 40% compared with other aircraft, although the battery power output does not exceed 10% of the total power delivered ($\Phi < 0.10$). The battery-assisted *SMR-boosted* configuration is not considered in the rest of the result analysis, in order to allow a finer comparison between aircraft closer to each other performance-wise.

Evolutions in PREE with harmonic range follow a pseudo-linear decreasing trend. That starkly differs from the case of regional aircraft which, over the interval of harmonic range considered, are curved around a local optimum, see fig.6. SMR aircraft with increasing design range are therefore getting less efficient per kg.km flown on their harmonic mission, the benefits associated with a longer cruise phase relative to the harmonic range being overshadowed by an increase in OEM. For the highest considered value in harmonic range (5010 km), the *SMR-baseline* aircraft has a PREE around 1.32, to be compared against that of the *LPA-baseline* aircraft around 1.52 at the lowest part of the LPA range (6480 km) see fig.9. Therefore, the current trend of expanding the harmonic range of A320-class aircraft towards long range values seems especially inappropriate from a climate impact point of view.

Figure 8 clearly indicates that radical configurations hardly manage to perform within 5%-10% of the baseline aircraft on a PREE basis. A difference with the regional class is that the hydrogen direct-burn *SMR-LH2* aircraft manages to achieve a lower MTOM than the *SMR-baseline*, suggesting that the lower fuel mass permitted by the higher gravimetric energy density of hydrogen outweighs the penalties associated with the presence of a LH2 tank and with its integration (extended fuselage).

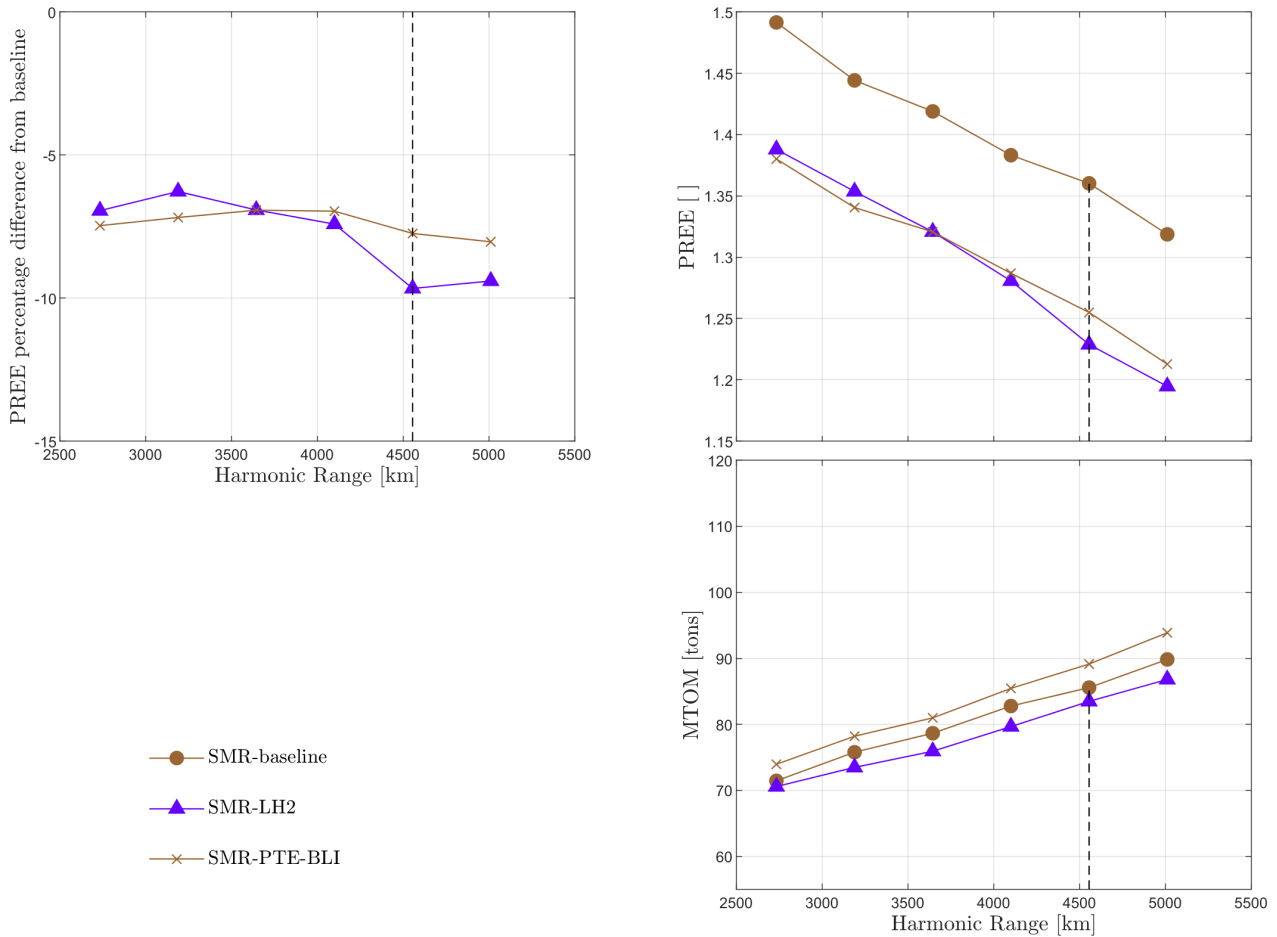


Figure 8 – Variations in MTOM and PREE with harmonic range. The vertical dashed line indicates the initial range value.

3.3 Large Passenger Aircraft Aircraft

On the LPA aircraft class, MTOM and PREE exhibits symmetrically opposed trends, with MTOM following a polynomial growth with increasing harmonic range, see fig.9. The efficiency of the *LPA-baseline* aircraft per kg.km flown hence displays a near 20% decrease over an harmonic range from 6500 km to almost 12000 km.

The *LPA-PTE-BLI* configurations manages to exceed the PREE of the *LPA-baseline* over the entire range interval considered, albeit by a few percent only (< 5%). it should be noted that the *LPA-PTE-BLI* of maximum range did not converge for reasons that still need further analysis on our part. Even though not a clearly pronounced trend, it seems that the relative PREE benefits of the *LPA-PTE-BLI* are highest for lower ranges, which is a rather counter-intuitive result as the BLI should provide an improvement in aero-propulsive efficiency, which typically is only exceeding the associated mass penalty over larger ranges.

Similar to the SMR class, the *LPA-LH2* aircraft has a lower MTOM than the *LPA-baseline* over the whole range, yet fails approximately 10% short in terms of PREE performance, with the biggest penalty at the highest range. This can be explain by the lower wing loading of the *LPA-LH2* aircraft, due to a higher landing mass fraction that makes the landing constraint more restrictive on the maximum feasible wing loading. A different wing loading directly affects lift coefficient in cruise, such that the lift over drag ratio can be negatively affected. This suggests to try a different cruise altitude for hydrogen-powered aircraft. Besides, a lower feasible wing loading also entails a larger wing mass for a given maximum take-off weight, which also affects the overall performance of the *LPA-LH2*.

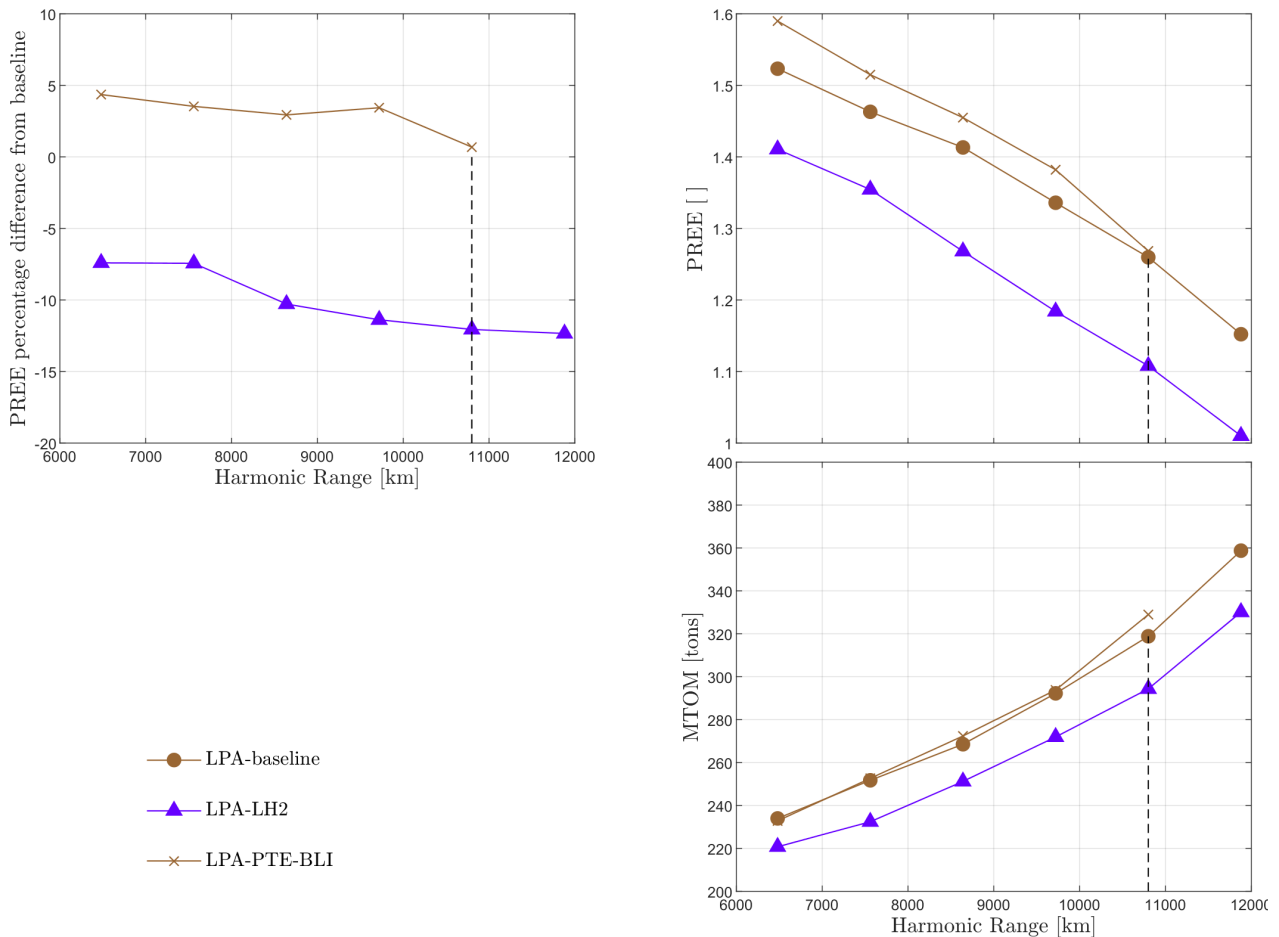


Figure 9 – Variations in MTOM and PREE with harmonic range. The vertical dashed line indicates the initial range value.

4. Passenger-Payload Exploration

4.1 Regional Aircraft

Un-surprisingly, the fuel-cell aircraft *REG-FC* is at much an outlier along the different passenger capacity, see fig.10, as it is along the different harmonic ranges. It is once again chosen not to consider it in the following analysis.

The variation in MTOM with a relative increase in passenger capacity (and associated payload) is much more pronounced than with a relative increase in harmonic range. It can be seen from fig.6 and fig.11 that MTOM increases by nearly 10% when the harmonic range more than doubles, while it increases by approximately 80-90% when the passenger capacity doubles.

None of the radical aircraft manage to reach the same PREE as the *REG-baseline*, and the penalty is especially pronounced for aircraft equipped with battery. The hydrogen direct-burn aircraft displays a decreasing relative penalty in PREE, compared to the baseline, with increasing passenger capacity. This can be explained by a relatively lower increase in fuselage length required to fit the LH2 tank, which translates into relatively lower penalties in OEM and fuselage drag. An increase in fuselage width, from a 4-abreast seating to a 5-abreast, may be particularly beneficial to the *REG-LH2* aircraft by offering a more spherical volume for the integration of the liquid hydrogen tank.

Overall, despite the increase in MTOM, the PREE increases with passenger capacity, such that large turboprop aircraft should offer a competitive energy consumption per pax.km flown.

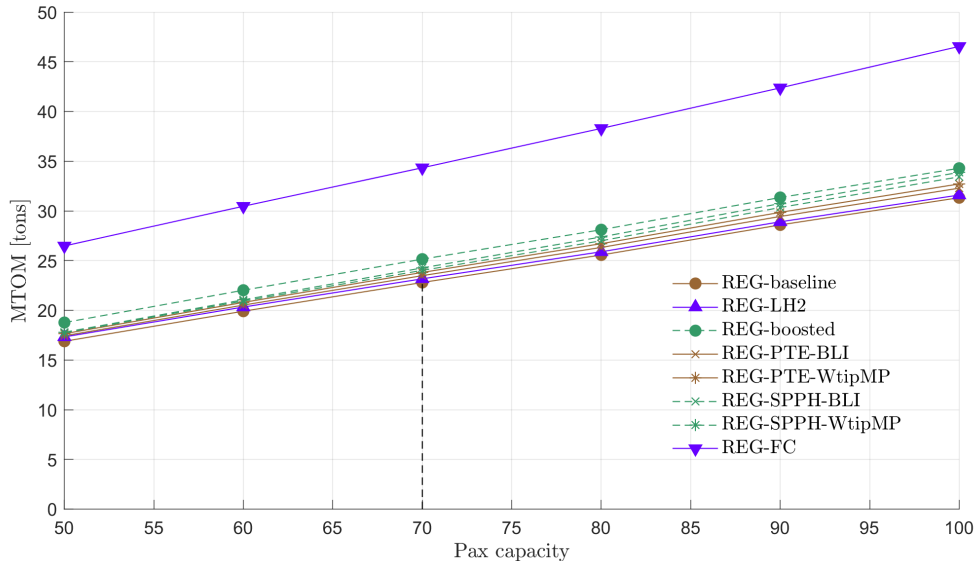


Figure 10 – Evolution of MTOM with passenger capacity for the regional class. The vertical dashed line indicates the initial passenger capacity.

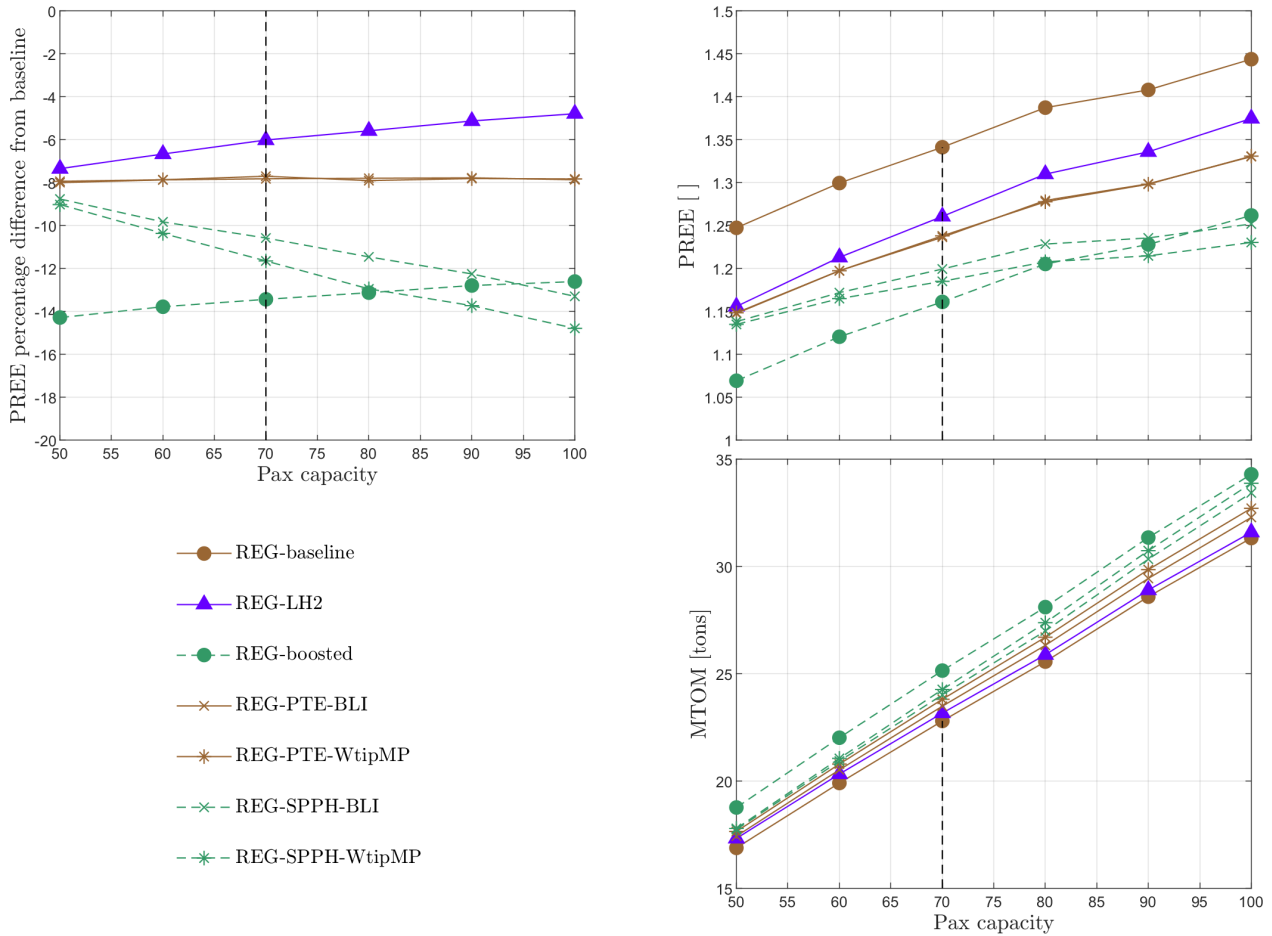


Figure 11 – Variations in MTOM and PREE with passenger capacity. The vertical dashed line indicates the initial passenger capacity.

4.2 Short-Medium Range Aircraft

The exploration in passenger capacity for the SMR class saw one iteration of the *SMR-boosted* aircraft not converge (122 passengers), which is surprising considering that passenger capacities above and below produced feasible aircraft. Besides, for that same passenger capacity, the sizing of the *SMR-baseline* and of the *SMR-PTE-BLI* also seems problematic: their MTOM and PREE values seem to be off the trend displayed by the *SMR-LH2*, see fig.13. This matter is the subject of ongoing work with the *Initiator*. Anyway, the MTOM of *SMR-boosted* aircraft far outweighs that of any other aircraft, as can be displayed in fig.12 such that it can not be considered a viable option.

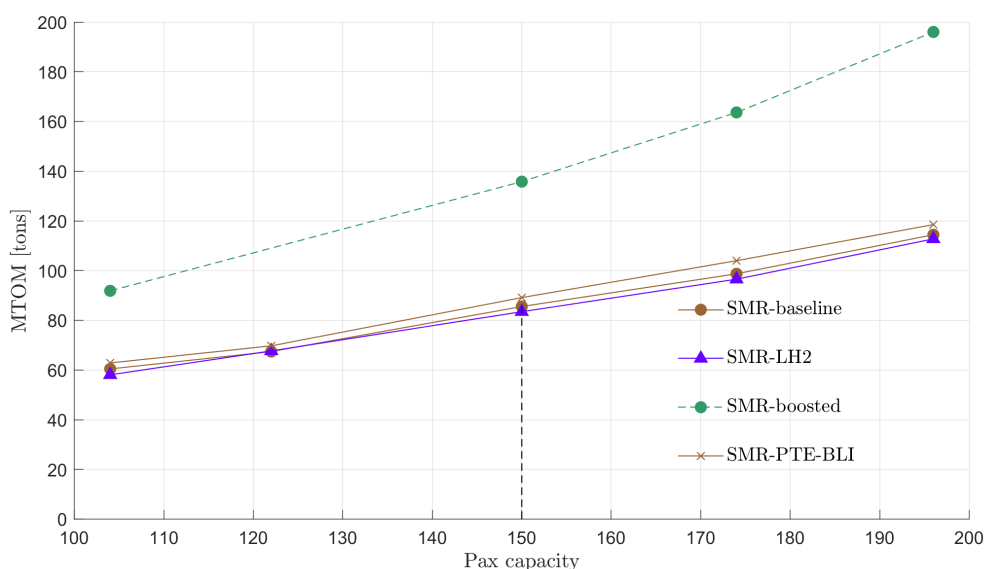


Figure 12 – Evolution of MTOM with passenger capacity for the Short-Medium Range class. The vertical dashed line indicates the initial passenger capacity.

Apart from a clear trend in increasing MTOM with passenger capacity, with the MTOM almost doubling when the capacity is doubled, the evolution in PREE lacks a clear trend. At the maximum passenger capacity considered in this study, the fuselage slenderness is quite extreme with the current 6-abreast seating configuration, which would negatively affect the fuselage mass. This is especially true for the *SMR-LH2* aircraft that needs to integrate a voluminous fuel tank aft of the passenger cabin. That being said, the *SMR-LH2* still does manage to reach a lower MTOM than the *SMR-baseline*.

Despite the *SMR-PTE-BLI* being the heaviest, it manages a better PREE than the *SMR-LH2* over the whole interval. That can partly be explained by the wing efficiency deficit that the *SMR-LH2* may experience by flying at an altitude that does not enable it to reach the optimum lift coefficient given its lowest wing loading.

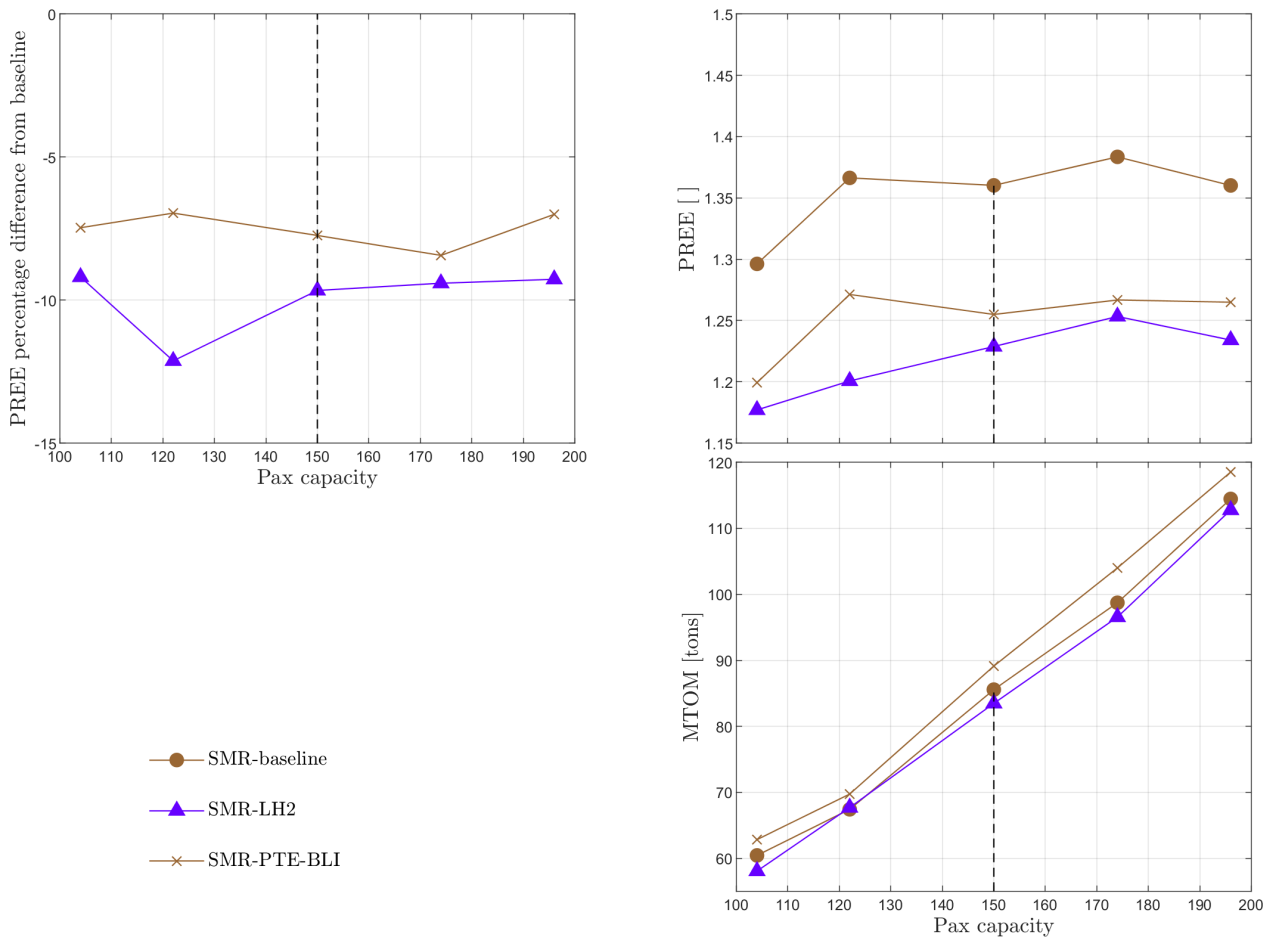


Figure 13 – Variations in MTOM and PREE with passenger capacity. The vertical dashed line indicates the initial passenger capacity.

4.3 Large Passenger Aircraft Aircraft

For large passenger aircraft, an increase in passenger capacity translates into a pseudo-linear increase in MTOM, almost following the same relative evolution. The *LPA-PTE-BLI* exhibits MTOM and PREE values for the 315 passenger capacity that seem somewhat off the otherwise linear trends. Nevertheless, overall the *LPA-PTE-BLI* manages to exceed the PREE of the *LPA-baseline* over the whole interval considered, and gets relatively better with increasing passenger capacity. That may be explained by the lengthened fuselage, which therefore sees a thicker boundary layer that dissipates more power. That trend is not so apparent for the SMR class however and should be the subject of more attention. Besides, the BLI aero-propulsive model uses a simplified geometrical representation of the fuselage and assumes a given boundary layer mean velocity profile. However, the subtleties brought by a real-world application, such as non-uniform inflow, can easily change the simplified picture assumed currently and significantly alter the corresponding aero-propulsive improvement. Once again, the *LPA-LH2* manages to reach the lowest MTOM, by quite some margins (approximately -10%) but nonetheless fails to come with 10% of the *LPA-baseline* PREE. The *LPA-LH2* and *LPA-PTE-BLI* call for conflicting trends in fuselage width: the former would take advantage of a larger cross-section, while the latter likely thrives with long fuselage. In future studies, it may be more consistent to compare those two configurations based on their respective optimized fuselage width. As the abreast seating combinations are anyway limited for twin aisle aircraft to 2-3-2, 2-4-2, 3-3-3 or 3-4-3, the design space is rather limited.

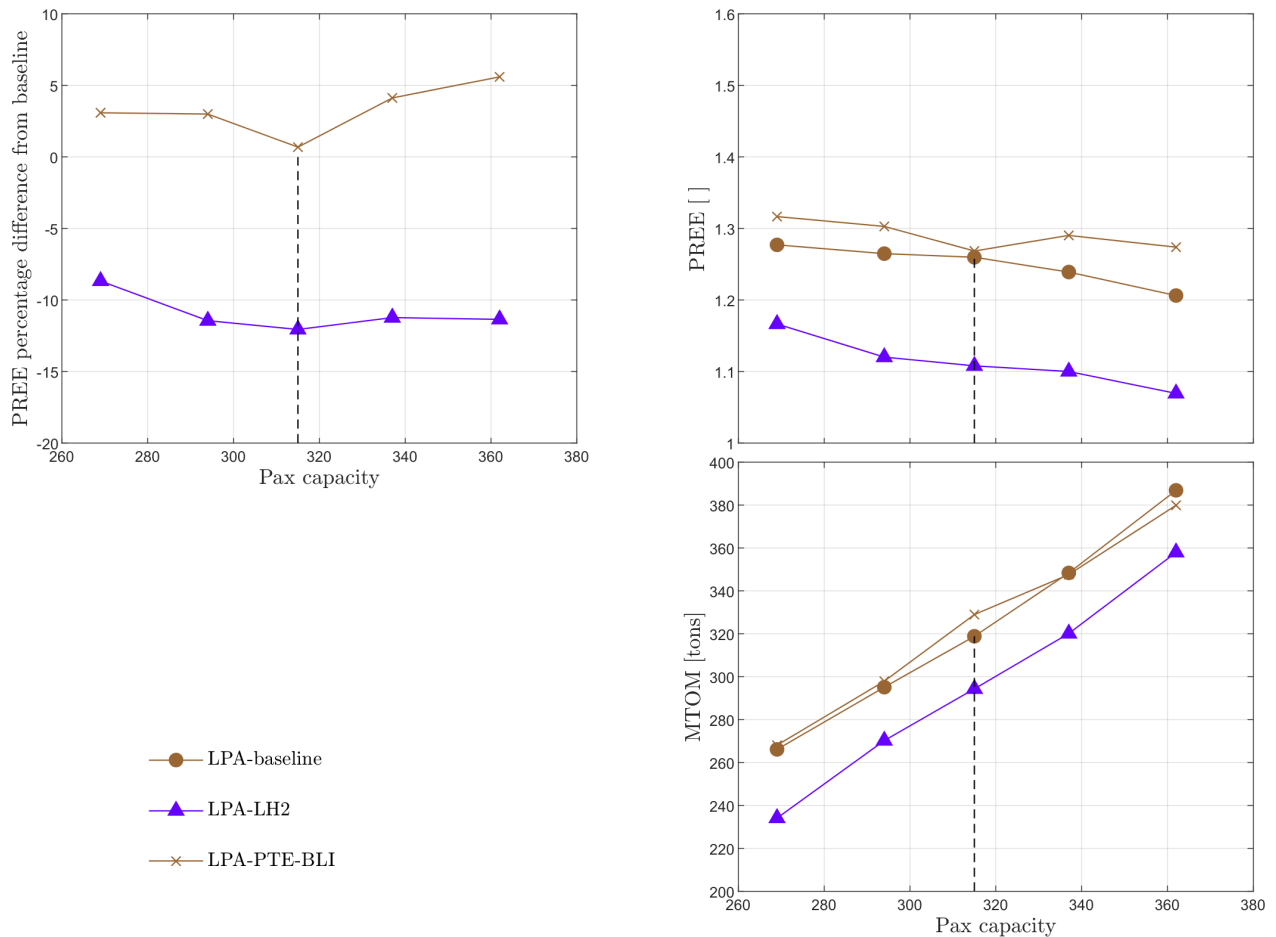


Figure 14 – Variations in MTOM and PREE with passenger capacity. The vertical dashed line indicates the initial passenger capacity value.

5. Conclusions

This article presents the sensitivity of a selection of radical design to variations in harmonic range and passenger capacity, for three classes of aircraft: regional, short-medium range and large passenger aircraft. The technology combinations are class-specific, albeit some are repeated over different classes, but they all include a so-called *baseline* aircraft of conventional architecture which is exposed to the TLARs. Even though radical designs configurations can still be fine-tuned and the preliminary sizing tool used improved, some early conclusions can still be drawn.

A first conclusion is that none of the radical aircraft configurations considered is able to achieve any breakthrough improvement in performance that would justify, from a technical point-of-view only, a trivial market switch towards hybrid-electric aircraft or hydrogen-powered aircraft. Only in few cases, radical aircraft are able to come close to the performance metrics set by the *baseline* or exceed it by a few percent, which falls within the percentage error of the methodology.

In particular, designs that include fuel-cells with their required supporting batteries seem too heavy to show any potential, even on the smaller regional aircraft considered here. Overall, aircraft equipped with batteries also suffer from an excessive take-off mass with a direct penalty on their payload-range efficiency, even though the battery supplied power ratios are kept below 10% and only applied during climb. If electrically-assisted turboprop or turboprop in a serial configuration show little promising perspective, SPPH powertrains should, at regional scale, be re-worked from their current state to explore the following options: explore combinations in supplied power ratio and shaft power ratio to find an optimum in terms of efficiency per kg.km flown, have the battery recharged by the GT turbine during descent only to avoid the over-sizing problem encountered here, or consider a 'plug-in' hybrid were the battery is charged on the ground.

Partial turbo electric configurations seem more promising in their potential to reach or exceed the performance of baseline configurations, this calls for a fine-tuning in supplied power ratio and span fraction of the distributed propulsion that should be done via a sensitivity analysis on those. For boundary-layer ingestion, another variable concerns the length of the fuselage, which can be changed by adapting the cabin layout and would have an impact on fuselage mass and aero-propulsive benefits of the BLI system.

Fuselage width should also particularly affect the sizing and integration of liquid hydrogen tank, such that this design variation should be explored for a given passenger capacity. Aircraft that use hydrogen in a conventional direct-burn configuration seems to offer the more realizable scenario towards a lower aviation CO₂ emissions, providing that the hydrogen used has a low carbon footprint. All the more as there is potential room for improvement, by adapting the cruise altitude to the lower wing loading achieved by 'LH2' aircraft in order to optimize their wing efficiency. However, their associated performance metrics are at best comparable to those of conventional Jet-A powered aircraft, such that the market shift towards such aircraft will likely have to be politically-driven.

The range and passenger capacity exploration is also providing interesting insights about baseline aircraft configurations, outlining that turboprop of larger passenger capacity and wide-body aircraft of shorter ranges could provide a significant reduction in emissions per kg.km flown at network level, if market compatible.

Finally, results obtained in this study are highly dependent on the relying technology assumptions. To ensure that radical designs are credible, the uncertainty of those assumptions should be quantified, and perhaps assumptions that correspond to a more credible scenario in technological improvements must be adopted.

Contact Author Email Address

You can contact the author at the following email address: v.o.bonnin@tudelft.nl

Copyright Statement

The authors confirm that they, and/or their company or organization, hold copyright on all of the original material included in this paper. The authors also confirm that they have obtained permission, from the copyright holder of any third party material included in this paper, to publish it as part of their paper. The authors confirm that they give permission, or have obtained permission from the copyright holder of this paper, for the publication and distribution of this paper as part of the ICAS proceedings or as individual off-prints from the proceedings.

Acknowledgements

Research presented in this publication was performed under the CHYLA project. This project has received funding from the European Union's Horizon 2020 research and innovation programme under grant agreement No. 101007715. The authors would like to thank CHYLA project participants for joint work sessions on the preliminary down-selection of technological combinations, particularly Mr. Nicolas Wahler and Mr. Lukas Radomsky for their inputs regarding the technology scenarios. Additionally, we would like to thank Dr. Reynard de Vries for his valuable inputs for the sizing (process) of hybrid electric aircraft and Ir. Giuseppe Onorato for his contributions to the aircraft designs.

References

- [1] V. Grewe, A. G. Rao, T. Grönstedt, C. Xisto, F. Linke, J. Melkert, J. Middel, B. Ohlenforst, S. Blakey, S. Christie, S. Matthes, and K. Dahmann. Evaluating the climate impact of aviation emission scenarios towards the paris agreement including COVID-19 effects. *Nature Communications*, 12(1), June 2021.
- [2] Advisory Council for Aeronautical Research in Europe (ACARE). European Aeronautics: a Vision for 2020. Technical report, 2001.
- [3] European Commission, Directorate-General for Mobility and Transport, Directorate-General for Research and Innovation. Flightpath 2050: Europe's Vision for Aviation. Technical report, 2011.

- [4] M. Hoogreef, R. Vos, R. de Vries, and L. L. Veldhuis. Conceptual assessment of hybrid electric aircraft with distributed propulsion and boosted turbofans. In *AIAA Scitech 2019 Forum*. American Institute of Aeronautics and Astronautics, Jan. 2019.
- [5] R. de Vries, M. Hoogreef, and R. Vos. Preliminary sizing of a hybrid-electric passenger aircraft featuring over-the-wing distributed-propulsion. In *AIAA Scitech 2019 Forum*, 2019.
- [6] M. Hoogreef and V. Bonnin. Scalability analysis of radical technologies to various aircraft class - part i: initial designs. In *ICAS 2022 Conference, 2022*. Submitted for Publication.
- [7] R. Elmendorp, R. Vos, and G. La Rocca. A conceptual design and analysis method for conventional and unconventional airplanes. In *Proceedings of ICAS 2014*, 2014.
- [8] M. Hoogreef, R. de Vries, T. Sinnige, and R. Vos. Synthesis of aero-propulsive interaction studies applied to conceptual hybrid-electric aircraft design. In *AIAA Scitech 2020 Forum*, 2020.
- [9] G. Onorato, P.-J. Proesmans, and M. F. M. Hoogreef. Assessment of hydrogen transport aircraft effects of fuel tank integration. *CEAS Aeronautical Journal*, 2022. Under Review.
- [10] D. Juschus. *Preliminary Propulsion System Sizing Methods for PEM Fuel Cell Aircraft*. Master's thesis, TU Delft Aerospace Engineering, 2021.
- [11] M. R. van Holsteijn, A. Gangoli Rao, and F. Yin. Operating characteristics of an electrically assisted turbofan engine. In *Turbo Expo: Power for Land, Sea, and Air*, volume 84058. American Society of Mechanical Engineers, 2020.
- [12] R. Nederlof. *Improved modeling of propeller-wing interactions with a lifting-line approach*. Master's thesis, TU Delft Aerospace Engineering, 2020.
- [13] Q. V. der Leer and M. Hoogreef. Aero-propulsive and aero-structural design integration of turbo-prop aircraft with electric wingtip-mounted propellers. In *AIAA SCITECH 2022 Forum*. American Institute of Aeronautics and Astronautics, Jan. 2022.
- [14] R. de Vries, M. T. Brown, and R. Vos. A preliminary sizing method for hybrid-electric aircraft including aero-propulsive interaction effects. In *2018 Aviation Technology, Integration, and Operations Conference*, 2018.
- [15] E. Torenbeek. *Advanced Aircraft Design: Conceptual Design, Technology and Optimization of Subsonic Civil Airplanes*. Wiley, 2013.
- [16] A. Isikveren, S. Kaiser, C. Pernet, and P. Vratny. Pre-design strategies and sizing techniques for dual-energy aircraft. *Aircraft Engineering and Aerospace Technology*, 86(6):525–542, Sept. 2014. R. Singh, editor.
- [17] R. de Vries, M. Hoogreef, and R. Vos. Aero-propulsive efficiency requirements for turboelectric transport aircraft. In *AIAA Scitech 2020 Forum*, 2020.